Journal of the European Ceramic Society 21 (2001) 1371–1375
www.elsevier.com/locate/jeurceramsoc

Effects of strontium substitution in Nb-doped PZT ceramics

H. Zheng[a,*], I.M. Reaney[a], W.E. Lee[a], N. Jones[b], H. Thomas[b]

[a]*Department of Engineering Materials, University of Sheffield, Sheffield S1 3JD, UK*
[b]*Morgan Electro Ceramics, Vauxhall Industrial Estate, Ruabon, Wrexham LL14 6HY, UK*

Received 4 September 2000; accepted 23 October 2000

Abstract

Nb-doped lead zirconate titanate (PZT) compositions (2.4 mol%) close to the morphotropic phase boundary (MPB) were investigated systematically as a function of Sr doping as well as Zr:Ti ratio. Sr substitution for Pb in PZT shifted compositions away from the MPB toward the tetragonal phase, greatly reducing the Curie temperature and broadening the dielectric constant maximum, but also decreasing the d_{33}. TEM studies revealed intragranular inhomogeneity in the domain structure with widths varying from ~100 to ~20 nm. Altering the Zr:Ti ratio back toward the MPB reduced the Curie temperature and increased the d_{33}. The d_{33} was optimised in a slightly tetragonal phase close to, but not exactly at, the MPB. © 2001 Elsevier Science Ltd. All rights reserved.

Keywords: Electron microscopy; Piezoelectric properties; PZT; Sensors and actuators

1. Introduction

Lead zirconate titanate (PZT) has the perovskite structure (general formula, ABO_3) with the A-site (Pb^{2+}) occupying the cubo-octahedral interstices described by the BO_6-site octahedra. At room temperature all compositions are ferroelectric when the Zr:Ti ratio $<95:5$. Above the Curie temperature, the unit cell is cubic, but below, it is distorted to either tetragonal (Zr:Ti$<53:47$) or rhombohedral (Zr:Ti$>53:47$). The boundary between these two phases (Zr:Ti ~53:47 at room temperature) is known as the morphotropic phase boundary (MPB).[1]

Modified PZT compositions find many applications in piezoelectric sensors, actuators and electromechanical transducers.[2] High values of piezoelectric coefficient d_{33} (>300 pC/N) in poled PZT are believed to arise from the motion of domain walls under the action of applied field or stress. This behaviour is termed 'soft'.[3] Several mechanisms are thought to promote domain wall motion in PZTs:

1. donor doping such as Nb^{5+} on the B-site,[4,5]
2. proximity to the MPB,[6] and
3. reducing the phase transition temperature by substituting, e.g. Sr^{2+} for Pb^{2+} on the A-site.[7]

In this study, 2.4 mol% Nb-doped soft PZTs were investigated systematically as a function of Sr content as well as Zr:Ti ratio. X-ray diffraction (XRD) was used to reveal any structural changes. Domain structures were monitored using transmission electron microscopy (TEM).

2. Experimental

Polycrystalline ceramic materials were obtained using reagent-grade raw materials: PbO, ZrO_2, TiO_2, Nb_2O_5 and $SrCO_3$. Starting reagents in the appropriate ratios plus 2 wt.% excess PbO were attrition-milled, and calcined at 925°C for 4 h. The calcined powder was attrition-milled again with 2 wt.% Carbowax PEG 10K added as a binder. The powder was dried at 60°C for 48 h, sieved through a 180 μm nylon sieve and then pressed into 10 mm diameter discs. Sintering was conducted in a lead-rich environment (pellets were embedded in $PbZrO_3$ powder) in the temperature range from 1140 to 1220°C for 4 h depending on composition. All the sintered samples have relative densities above 95%.

XRD patterns were recorded in the scan range 2θ of 20–60° on a Philips 1700 diffractometer with CuK_α source. Indices of the XRD peaks are based on a pseudocubic cell.

Samples for TEM were first ground flat to ~25 μm and then ion milled until perforation. Specimens were

---

[*] Corresponding author. Tel.: +114-222-5990; fax: +114-222-5943.
E-mail address: mtp98hz@sheffield.ac.uk (H. Zheng).

PII: S0955-2219(01)00021-8

coated with carbon before examination using Philips 420 TEM, operating at 120 kV.

Capacitance as a function of temperature was measured on a HP 4284A LCR meter at a frequency of 1 kHz. The LCR meter was used in conjunction with a computer-controlled temperature chamber. Capacitance was converted to relative permittivity using the sample geometry and the permittivity of air.

Samples for d_{33} testing were poled in insulation oil at 130°C for 3 min at a field strength of 2 kV/mm. Measurements were then performed, 24 h after the poling, using a Piezometer System PM 2C at a frequency of 100 Hz.

3. Results and discussion

3.1. Effect of Sr content

Fig. 1 shows XRD patterns from 2.4 mol% Nb-doped PZT samples (Zr:Ti ratio: 1.095), in which the Sr is systematically substituted for Pb on the A-site. Samples containing less than 16 mol% Sr are tetragonal whereas with 32 mol% Sr, a pseudocubic pattern is observed. In samples with 0 mol% Sr, there is evidence for the presence of both rhombohedral and tetragonal phases, indicated by a shoulder on the 111 peak. As Sr content increases, the shoulder on the 111 peak disappears and tetragonal peaks become more intense.

Fig. 2 shows plots of relative permittivity versus temperature for the compositions in Fig. 1. The Curie temperature (T_C) reduces from 360 to 30°C by doping with up to 32 mol% Sr. For 32 mol% Sr samples, T_C is close to room temperature and therefore they appear pseudocubic, as ascertained by XRD (Fig. 1). In addition to decreasing the T_C, Sr broadens the phase transition maximum implying that the distribution of Curie temperatures is increased within the samples.

Although a decrease in the temperature of the relative permittivity maximum is observed (one of the mechanisms by which domain wall motion is made easier), the value of d_{33} diminishes as Sr increases (Fig. 3). It is proposed that increasing Sr on the A-site moves compositions away from the MPB, suggesting that controlling Zr:Ti ratio is more important to domain wall motion than simply reducing the phase transition temperature.

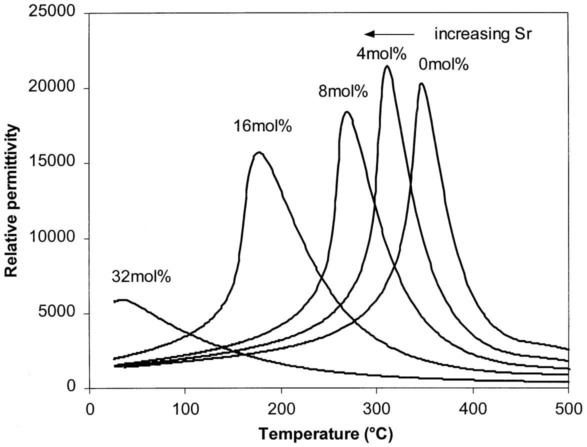

Fig. 2. Relative permittivities of 2.4 mol% Nb-doped PZT (Zr:Ti ratio: 1.095) as a function of Sr content.

Fig. 4 is a bright-field (BF) TEM image revealing domains (~100 nm wide), typical of 0% Sr-doped PZT. These domain walls lie on specific crystallographic planes and are characteristic of orientational or 90° domains.[8]

Similar domain structures are observed in samples containing Sr, but their width diminishes as dopant level increases. In addition, intragranular heterogeneity of the domain width is observed, an effect illustrated in Fig. 5 which shows ~100 nm as well as finer ~20 nm wide domains. The observation of regions with different domain structure implies a distribution of Sr concentration (and/or Zr:Ti ratio) even within a grain. This is consistent with the broadening of the relative permittivity maximum with increasing Sr content since in each case a distribution of Curie temperatures is implied.

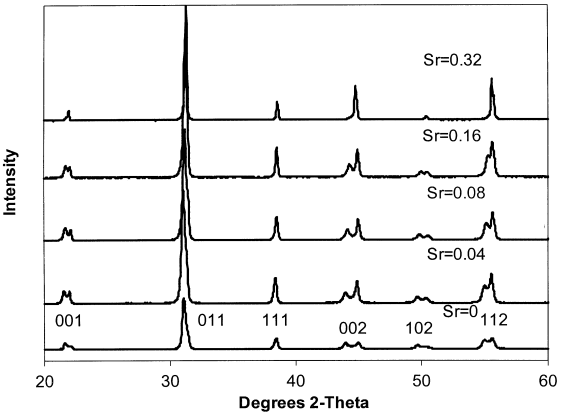

Fig. 1. XRD of 2.4 mol% Nb-doped PZT (Zr:Ti ratio: 1.095) as a function of increasing Sr content.

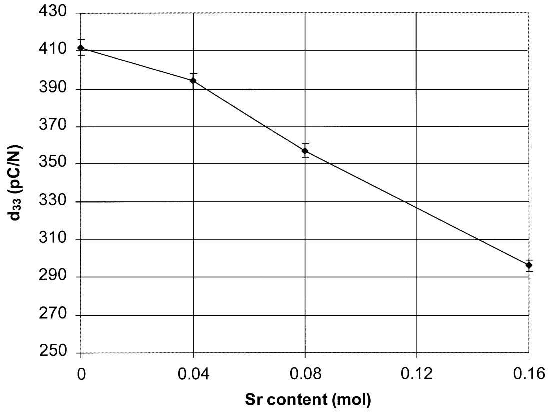

Fig. 3. d_{33} as a function of Sr content in 2.4 mol% Nb-doped PZT (Zr:Ti ratio: 1.095).

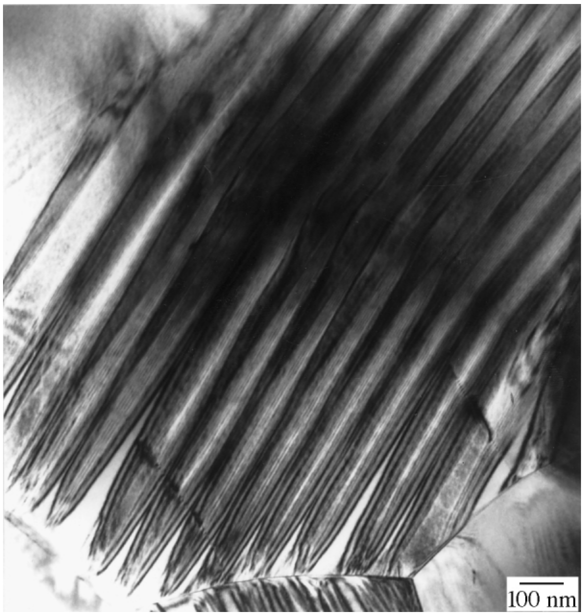

Fig. 4. Bright-field (BF) TEM image showing 90° domains in 2.4 mol% Nb-doped PZT (Zr:Ti ratio: 1.095).

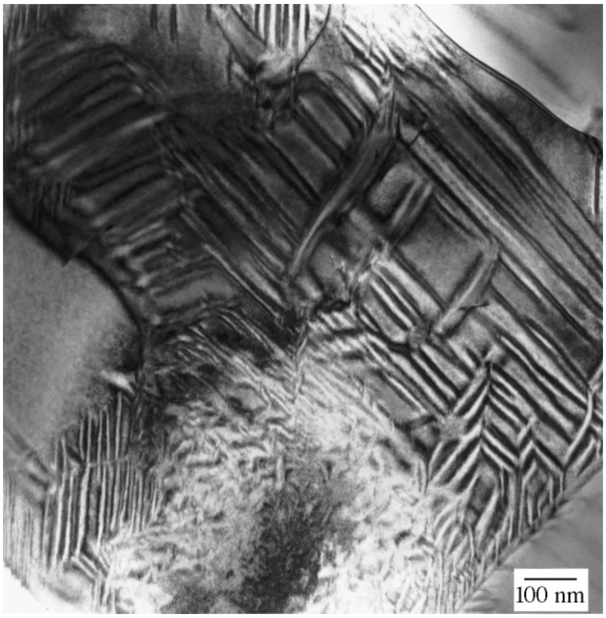

Fig. 5. BF TEM image showing fine scale domains in 16 mol% Sr-doped PZT (Nb: 2.4 mol%, Zr:Ti ratio: 1.095).

Fig. 6 reveals similar boundaries to those in Fig. 5, but walls with ribbon-like contrast are also present, typical of inversion (180°) domains.

3.2. *Effect of Zr:Ti ratio in 16 mol% Sr-doped PZTs*

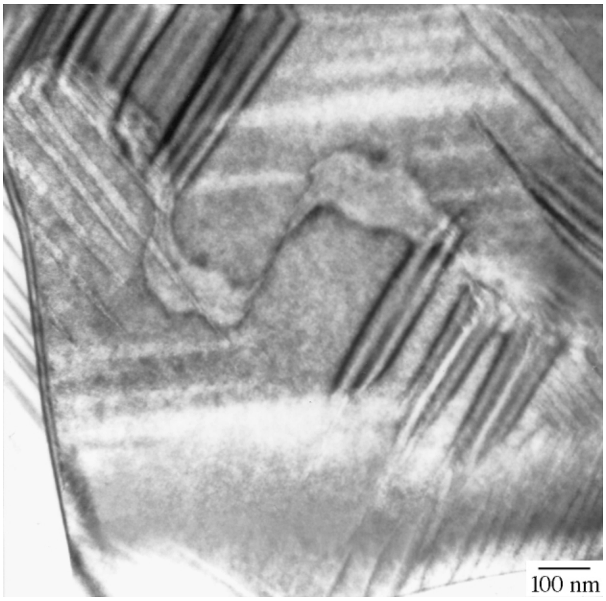

Fig. 6. BF TEM image showing an inversion domain boundary (arrowed) in 16 mol% Sr-doped PZT (Nb: 2.4 mol%, Zr:Ti ratio: 1.095).

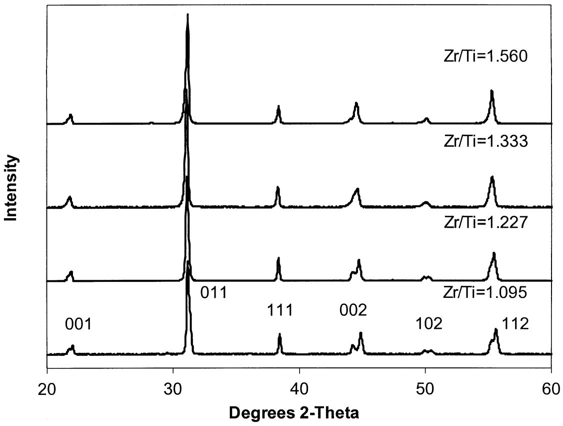

Fig. 7. XRD of 16 mol% Sr-doped PZTs with varying Zr:Ti ratio.

Fig. 7 shows XRD from 2.4 mol% Nb-doped PZT samples containing 16 mol% Sr on the A-site, in which, the Zr:Ti ratio has been varied to account for the increase in tetragonality observed in Fig. 1. As the Zr:Ti ratio increases, the peak splitting of 200 diminishes, indicating that samples have moved from a tetragonal to rhombohedral or mixed compositon across the MPB at the Zr:Ti ratio of 1.560.

Fig. 8 is a plot of relative permittivity versus temperature for the samples shown in Fig. 7. T_C decreases from 178 to 138°C as the Zr:Ti ratio increases from 1.095 to 1.560.

Fig. 9 illustrates the effect of changing Zr:Ti concentration on d_{33}. Initially d_{33} increases with Zr:Ti ratio reaching a maximum at 1.333. This can be explained by considering that phase composition moves closer to the MPB. However, the d_{33} for samples with Zr:Ti = 1.560 decreases with respect to the previous value. It is possible that this composition has moved to the rhombohedral side of the MPB and is no longer optimised for d_{33}. Furthermore, the Curie temperature for this composition is

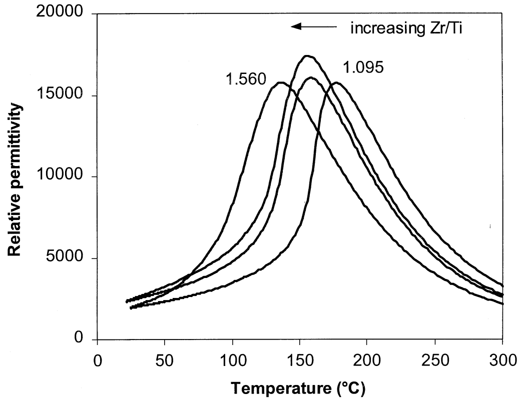

Fig. 8. Relative permittivities of 16 mol% Sr-doped PZT as a function of Zr:Ti ratio.

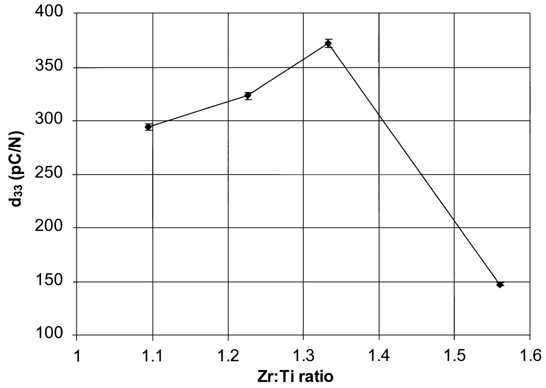

Fig. 9. d_{33} as a function of Zr:Ti ratio in 16 mol% Sr-doped PZT.

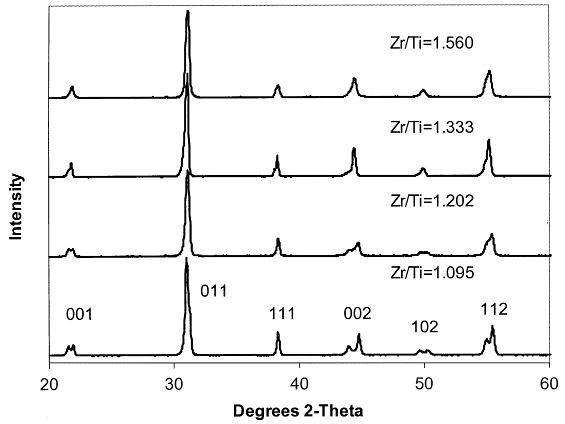

Fig. 10. XRD of 8 mol% Sr-doped PZT with varying Zr:Ti ratio.

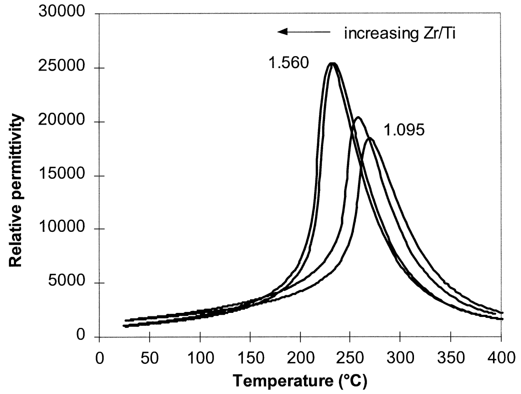

Fig. 11. Relative permittivities of 8 mol% Sr-doped PZT as a function of Zr:Ti ratio.

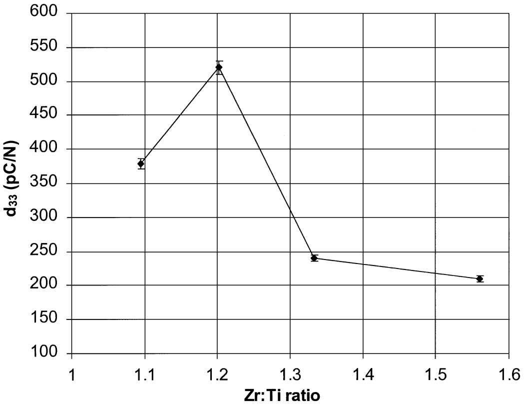

Fig. 12. d_{33} as a function of Zr:Ti ratio in 8 mol% Sr-doped PZT.

at 138°C and for consistency a poling temperature of 130°C has been used for these samples. Therefore, a significant portion of the Curie temperature is below the poling temperature (approximate 50%) and it is likely that the sample remains largely unpoled.

3.3. Effect of Zr:Ti ratio in 8 mol% Sr-doped PZTs

Fig. 10 reveals XRD from 2.4 mol% Nb-doped PZT containing 8 mol% Sr in which the Zr:Ti ratio has been varied in a similar manner as described in the previous section. A structural change is observed from tetragonal to mixed phase as the Zr:Ti ratio increases, as indicated by a change from 200 to mixed 111/200 peak splitting.

Fig. 11 is the associated dielectric data as a function of temperature. The same trend is observed as in Fig. 8 except here the Curie temperature decreases from 269 to 231°C when Zr:Ti ratio increases from 1.095 to 1.560.

Fig. 12 shows d_{33} values of the compositions shown in Fig. 10. d_{33} first increases with Zr:Ti ratio, which approaches a maximum (around 520 pC/N) at Zr:Ti = 1.202. This is attributed to the phase composition being moved closer to the MPB. The further decrease in d_{33} arises since the samples are moved to the rhombohedral side of the MPB. This confirms the observation in the previous section that the d_{33} is optimised in a slightly tetragonal phase rather than exactly at the MPB.

4. Conclusions

Sr doping in PZTs promotes the tetragonal over the rhombohedral phase for a fixed Zr:Ti ratio. The Curie temperature is greatly reduced but d_{33} still decreases suggesting that control of the Zr:Ti ratio is more important for the d_{33} than reducing the Curie temperature.

Domain width is finer in samples doped with Sr on the A-site. In addition the distribution of domain widths is inhomogeneous even within a grain, varying from ~100 to ~20 nm. This observation is consistent with the increased width of the relative permittivity maximum.

References

1. Gupta, S. M. and Viehland, D., Tetragonal to rhombohedral transformation in the lead zirconium titanate lead magnesium niobate-lead titanate crystalline solution. *J. Appl. Phys.*, 1998, **83**(1), 407–414.
2. Tan, Q. and Viehland, D., Influence of thermal and electrical histories on domain structure and polarization switching in potassium-modified lead zirconate titanate ceramics. *J. Am. Ceram. Soc.*, 1998, **81**(2), 328–336.
3. Fang, D. N. and Li, C. Q., Nonlinear electric-mechanical behavior of a soft PZT-51 ferroelectric ceramic. *J. Mater. Sci.*, 1999, **34**, 4001–4010.
4. Park, J. H., Kim, B. K. and Song, K. H., Piezoelectric properties of Nb_2O_5 doped and MnO_2–Nb_2O_5 co-doped $Pb(Zr_{0.53}Ti_{0.47})O_3$ ceramics. *J. Mater. Sci.*, 1995, **6**, 97–101.
5. Yoon, S. J., Effect of additives on the electromechanical properties of $Pb(Zr,Ti)O_3$–$Pb(Y_{2/3}W5_{1/3})O_3$ ceramics. *J. Am. Ceram. Soc.*, 1997, **80**(4), 1035–1039.
6. Randall, C. A., Kim, N., Kucara, J., Cao, W. and Shrout, T. R., Intrinsic and extrinsic size effects in fine-grained morphotropic-phase-boundary lead zirconate titanate ceramics. *J. Am. Ceram. Soc.*, 1998, **81**(3), 677–688.
7. Hench, L. L. and West, J. K., *Principles of Electronic Ceramics*. John Wiley & Sons, New York, 1990, p. 273.
8. Lee, W. E., Reaney, I. M. and McCoy, M. A., Planar defects in electroceramics. *British Ceramic Proceedings: 21st Century Ceramics,* 1996, No. 55, 199–212.